

30 Years of Box-Ball Systems

Atsuo Kuniba (Univ. Tokyo)

Rikkyo MathPhys 2022, 8 January 2022

Box-ball systems (BBS) brief chronicle

1990 First example by Takahashi-Satsuma

1996 Ultradiscretization

Classical integrability

1999 Connection to crystal base theory

Quantum (Yang-Baxter) integrability,

Quantum group theoretical generalizations,

Geometric crystals

2006 Combinatorial Bethe ansatz

Action-angle variables, KKR bijection, Fermionic formulas,

Solution of initial value problem

2018 Randomized BBS

Generalized Gibbs ensemble, Thermodynamic Bethe ansatz,

Limit shape of conserved Young diagrams

2019 Generalized hydrodynamics

Speed equation, Riemann problem,

Current fluctuations and large deviations

n -color Box-ball system (BBS)

$n = 3$ example.

... 00000000**33211**0000000000000000000000000000 ...
... 0000000000000**33211**00000000000000000000000000 ...
... 000000000000000**33211**000000000000000000000000 ...

0 = empty box, 1, 2, 3 = balls with colors

- time evolution = (move 1) · (move 2) · (move 3)

(move i) · Pick the leftmost ball with color i and move it to the nearest right empty box.

- Do the same for the other color i balls.

- soliton=consecutive balls $i_1 \dots i_a$ with color $i_1 \geq \dots \geq i_a \geq 1$.
- velocity=amplitude.

- Collisions of 2 solitons

- Amplitudes are individually conserved.

- Two body scattering:

Exchange of internal labels (colors) like quarks in hadrons

Phase shift

Collision of 3 solitons

... 003210031000020000000000000000 ...
... 000003210310002000000000000000 ...
... 000000003203110200000000000000 ...
... 000000000032003121000000000000 ...
... 00000000000032001032100000000 ...
... 000000000000003201000321000000 ...
... 00000000000000003021000032100 ...

Yang-Baxter relation is valid.

(Solitons in final state are independent of the order of collisions)

Double (classical and quantum) origin of integrability

(1) Ultra-Discretization (UD) of soliton equations

- Key formula

$$\lim_{\varepsilon \rightarrow +0} \varepsilon \log \left(\exp\left(\frac{a}{\varepsilon}\right) + \exp\left(\frac{b}{\varepsilon}\right) \right) = \max(a, b)$$

$$\lim_{\varepsilon \rightarrow +0} \varepsilon \log \left(\exp\left(\frac{a}{\varepsilon}\right) \times \exp\left(\frac{b}{\varepsilon}\right) \right) = a + b$$

$$(+, \times) \longrightarrow (\max, +)$$

keeps distributive law:

$$AB + AC = A(B + C) \rightarrow \max(a + b, a + c) = a + \max(b, c)$$

- UD of a discrete KdV equation gives an evolution equation of the $n = 1$ BBS (1996).

(2) Solvable lattice model at “ Temperature 0 ”

Time evolution pattern

... 031002000000 ...
... 000310200000 ...
... 0000031200000 ...
... 0000000132000 ...
... 0000000010320 ...

emerges from a configuration of a 2D lattice model in statistical mechanics

by forgetting the hidden variables on the horizontal edges.

- n -color box-ball system

= 2D solvable vertex model associated with quantum group

$$U_q(\widehat{sl}_{n+1}) \text{ at } q = 0 \quad (q \sim \text{temperature})$$

- Row transfer matrix at $q = 0$

= deterministic map (defined by the unique configuration surviving at $q = 0$)

= time evolution of box-ball system (forming a commuting family $T_1, T_2, \dots, T_\infty$)

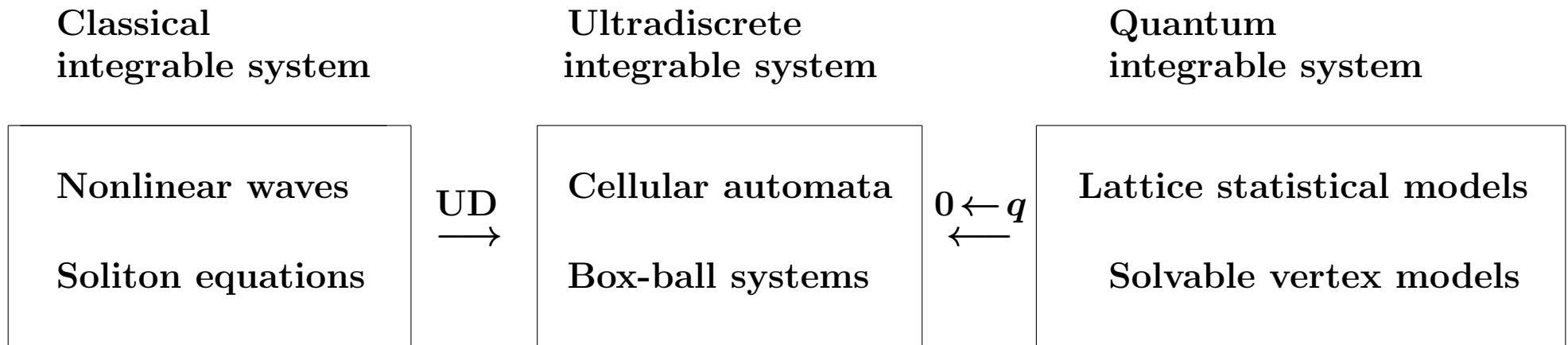
- Proper formulation uses *crystal base theory* (theory of quantum group at $q = 0$).

Some outcomes from such insight

- \exists Integrable cellular automata with quantum group symmetry.

Example: $\widehat{\text{so}}_{10}$ -automaton

- Particles and antiparticles undergo **pair-creations/annihilations**.
 - n -color BBS = \widehat{sl}_{n+1} -automaton = $\widehat{\text{so}}_{2n+2}$ -automaton in **antiparticle-free sector**.
 - Soliton & scattering most naturally captured in quantum group framework.



Inverse scattering method

KKR bijection

Bethe ansatz

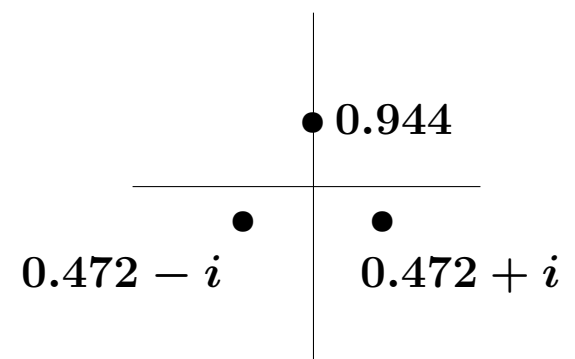
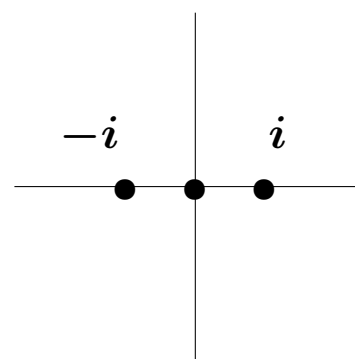
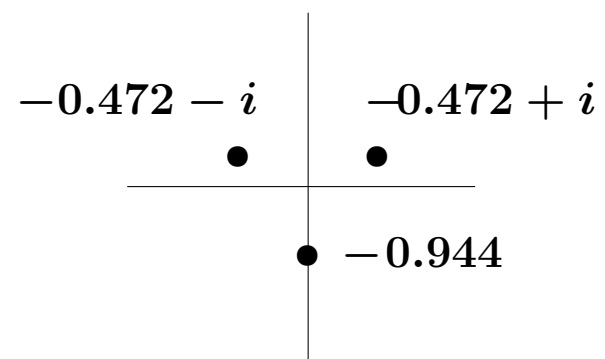
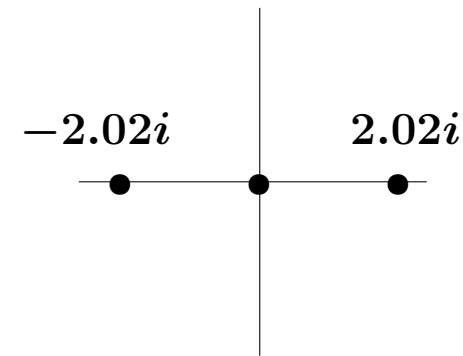
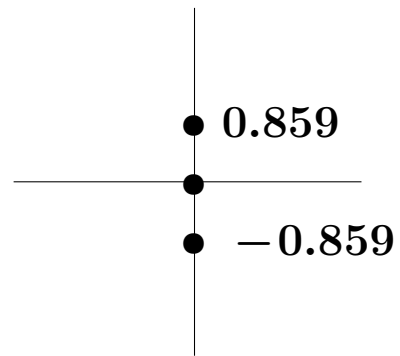
- **Kerov-Kirillov-Reshetikhin (KKR) bijection** (1986) asserts “formal completeness” of the hypothetical string solutions to the Bethe equation at combinatorial level.
- Its remarkable connection to BBS was discovered in 2002.

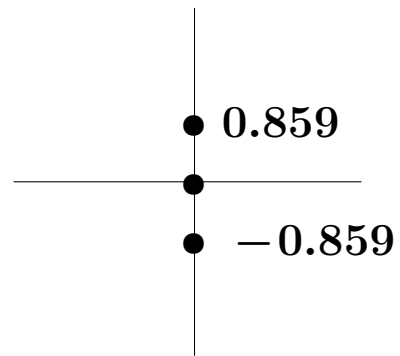
- Example. Spin $\frac{1}{2}$ periodic Heisenberg chain

$$H = \sum_{k=1}^L (\sigma_k^x \sigma_{k+1}^x + \sigma_k^y \sigma_{k+1}^y + \sigma_k^z \sigma_{k+1}^z - 1)$$

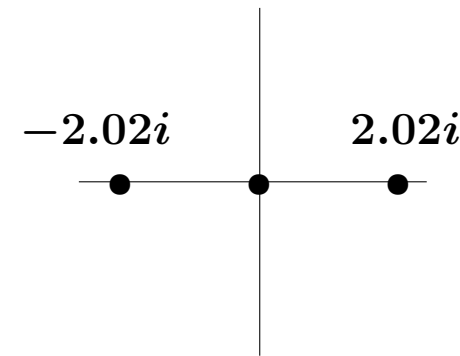
For $L = 6$ sites in 3 down-spin sector, the Bethe equation reads

$$\begin{aligned} \left(\frac{u_1 + i}{u_1 - i}\right)^6 &= \frac{(u_1 - u_2 + 2i)(u_1 - u_3 + 2i)}{(u_1 - u_2 - 2i)(u_1 - u_3 - 2i)}, \\ \left(\frac{u_2 + i}{u_2 - i}\right)^6 &= \frac{(u_2 - u_1 + 2i)(u_2 - u_3 + 2i)}{(u_2 - u_1 - 2i)(u_2 - u_3 - 2i)}, \\ \left(\frac{u_3 + i}{u_3 - i}\right)^6 &= \frac{(u_3 - u_1 + 2i)(u_3 - u_2 + 2i)}{(u_3 - u_1 - 2i)(u_3 - u_2 - 2i)}. \end{aligned}$$

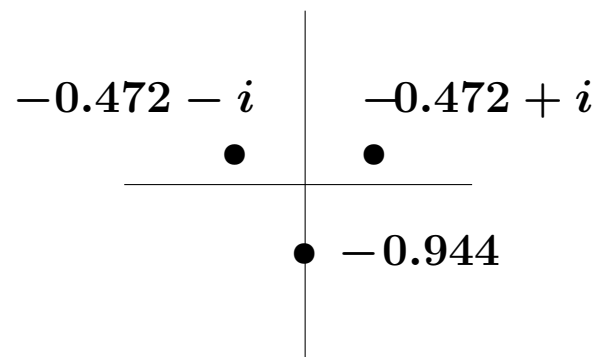




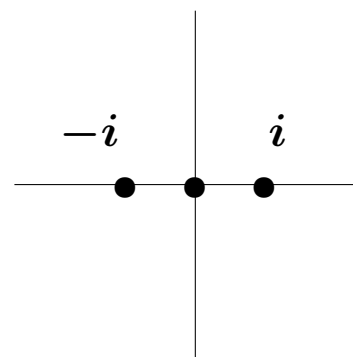
0
0
0



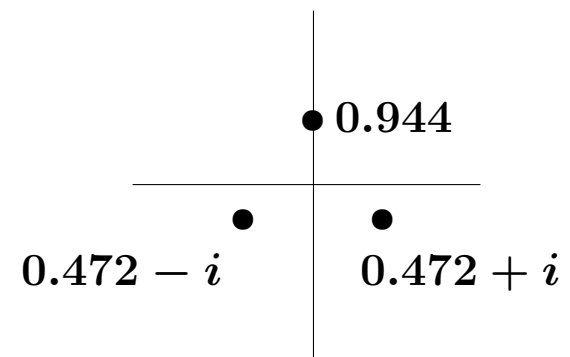
0



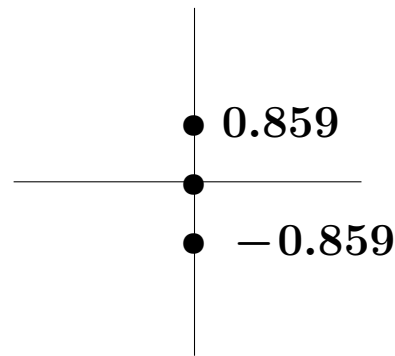
0
0



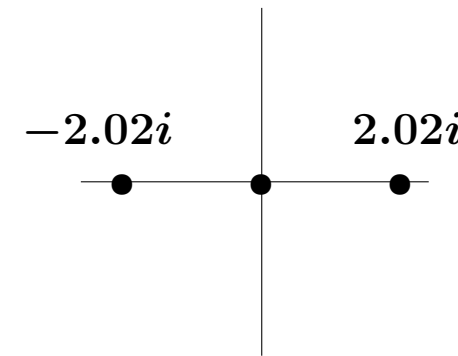
0
1



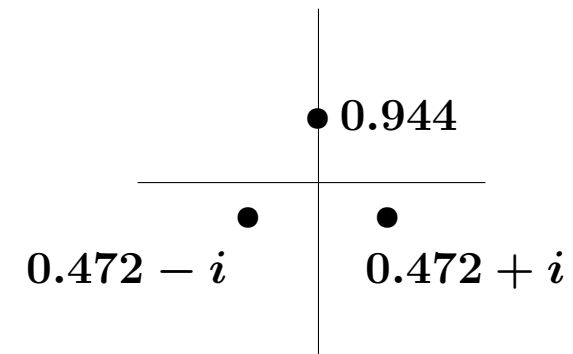
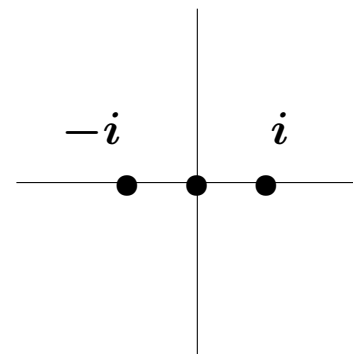
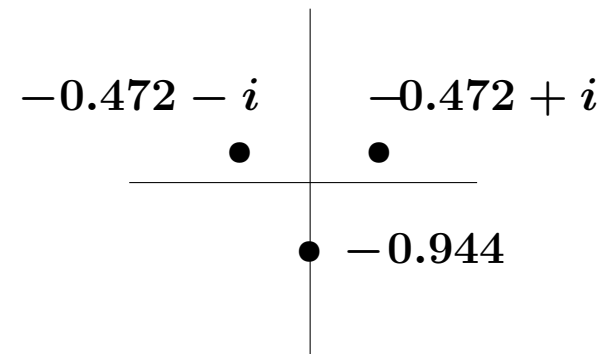
0
2



$$010101 \longleftrightarrow \begin{array}{|c|c|c|} \hline & & 0 \\ \hline & & 0 \\ \hline & & 0 \\ \hline \end{array}$$



$$000111 \longleftrightarrow \begin{array}{|c|c|c|} \hline & & \\ \hline & & \\ \hline & & 0 \\ \hline \end{array}$$



$$010011 \longleftrightarrow \begin{array}{|c|c|c|} \hline & & \\ \hline & & \\ \hline & 0 & \\ \hline \end{array} 0$$

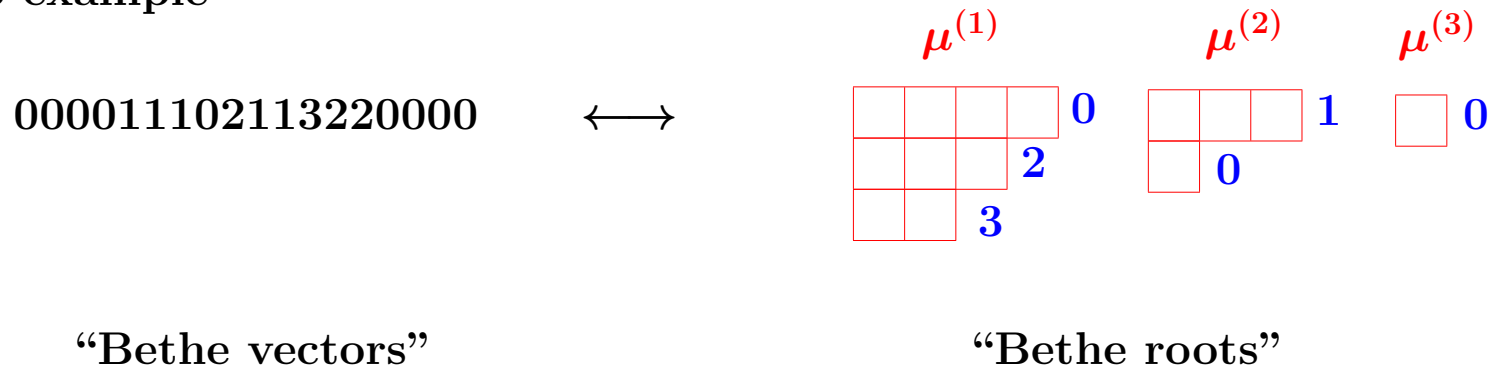
$$001011 \longleftrightarrow \begin{array}{|c|c|c|} \hline & & \\ \hline & & \\ \hline & 1 & \\ \hline \end{array} 0$$

$$001101 \longleftrightarrow \begin{array}{|c|c|c|} \hline & & \\ \hline & & \\ \hline & 2 & \\ \hline \end{array} 0$$

KKR bijection for sl_{n+1}

$$\{\text{highest states}\} \quad \xleftrightarrow{1:1} \quad \{\text{rigged configurations}\}$$

$n = 3$ example



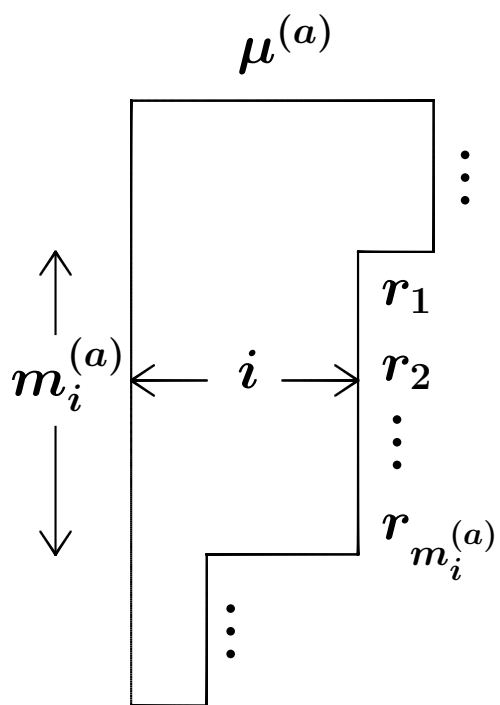
- highest states = $i_1 i_2 \dots i_L$ ($0 \leq i_k \leq n$) satisfying the highest condition:

$$\#_0\{i_1, \dots, i_k\} \geq \#_1\{i_1, \dots, i_k\} \geq \dots \geq \#_n\{i_1, \dots, i_k\} \quad (\forall k)$$

- rigged configuration: $((\mu^{(1)}, r^{(1)}), \dots, (\mu^{(n)}, r^{(n)}))$

$\mu^{(1)}, \dots, \mu^{(n)}$: configuration = n -tuple of Young diagrams
 $r^{(1)}, \dots, r^{(n)}$: rigging = integers assigned to each row

$\left. \right\} + \text{selection rule (next page)}$



$$m_i^{(a)} = \#(\text{length } i \text{ rows in } \mu^{(a)})$$

$$0 \leq r_1 \leq \cdots \leq r_{m_i^{(a)}} \leq h_i^{(a)}$$

... “Fermionic” selection rule

$$h_i^{(a)} = L\delta_{a,1} - \sum_{b=1}^n C_{ab} \sum_{j \geq 1} \min(i, j) m_j^{(b)}$$

... vacancy for *holes*

(C_{ab}) ... Cartan matrix of sl_{n+1}

$$\# \text{ of rigging choices for a fixed configuration} = \prod_{a=1}^n \prod_{i \geq 1} \binom{h_i^{(a)} + m_i^{(a)}}{m_i^{(a)}}$$

This is an sl_{n+1} generalization of Bethe’s formula for # of string solutions (1931), which yields the so-called Fermionic character formula for KR modules.

hat also eine Möglichkeit weniger, die des letzten Komplexes von n Wellen, λ_{q_n} , kann schließlich nur noch

$$Q'_n - (q_n - 1) = Q_n + 1$$

verschiedene Werte annehmen, wo

$$Q_n(N, q_1 q_2 \dots) = N - 2 \sum_{p < n} p q_p - 2 \sum_{p \geq n} n q_p. \quad (44)$$

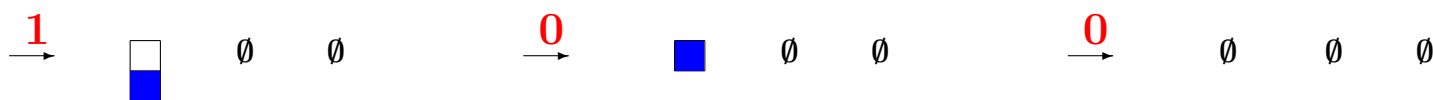
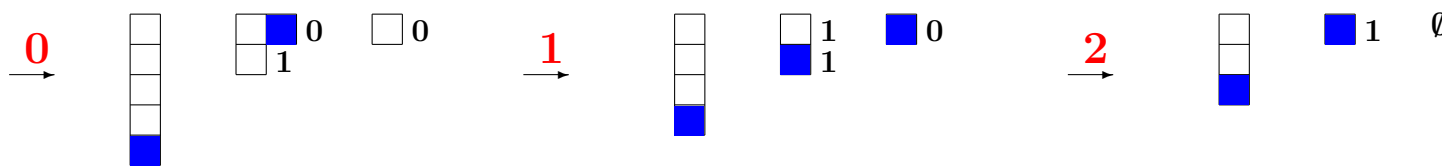
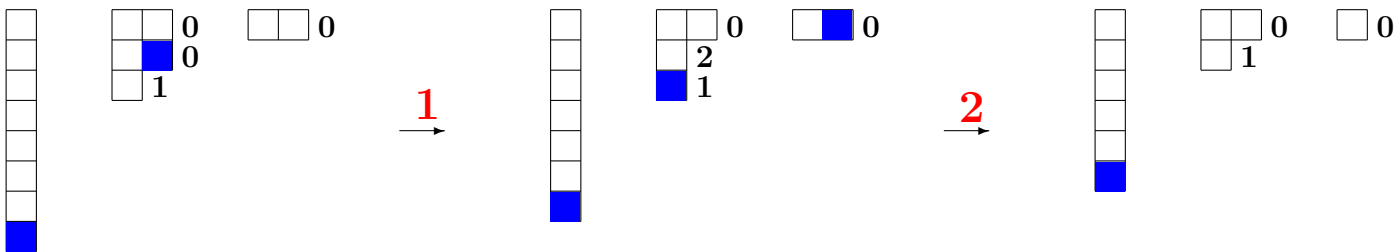
Schließlich ist zu berücksichtigen, daß Vertauschung der λ der verschiedenen Wellenkomplexe mit gleicher Anzahl n von Wellen nicht zu neuen Lösungen führt. Die gesamte Zahl unserer Lösungen wird somit

$$z(N, q_1 q_2 \dots) = \prod_{n=1}^{\infty} \frac{(Q_n + q_n) \dots (Q_n + 1)}{q_n!} = \prod_n \binom{Q_n + q_n}{q_n}, \quad (45)$$

wo die Q_n durch (44) definiert sind.

8. Wir werden nun nachweisen, daß wir die richtige Anzahl Lösungen erhalten haben.

Example of KKR algorithm



Top left rigged configuration $\xrightarrow{\text{KKR}}$ 00121021

How does the BBS dynamics look like in terms of rigged configurations ?

How does the BBS dynamics look like in terms of rigged configurations ?

$$\begin{array}{c}
 \xrightarrow{\text{KKR}} \quad \mu^{(1)} \quad \mu^{(2)} \quad \mu^{(3)} \\
 \begin{array}{|c|c|c|c|} \hline & & & \\ \hline & & & \\ \hline & & & \\ \hline \end{array} \quad 4t \\
 \begin{array}{|c|c|c|c|} \hline & & & \\ \hline & & & \\ \hline & & & \\ \hline \end{array} \quad 6 + 3t \\
 \begin{array}{|c|c|c|c|} \hline & & & \\ \hline & & & \\ \hline & & & \\ \hline \end{array} \quad 11 + 2t \\
 \begin{array}{|c|c|c|c|} \hline & & & \\ \hline & & & \\ \hline & & & \\ \hline \end{array} \quad 0
 \end{array}$$

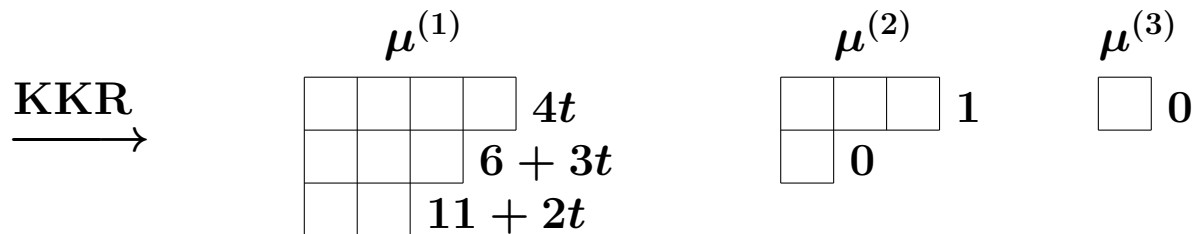
How does the BBS dynamics look like in terms of rigged configurations ?

$$\begin{array}{c}
 \xrightarrow{\text{KKR}} \quad \mu^{(1)} \quad \mu^{(2)} \quad \mu^{(3)} \\
 \begin{array}{|c|c|c|c|} \hline & & & \\ \hline & & & \\ \hline & & & \\ \hline \end{array} \quad 4t \\
 \begin{array}{|c|c|c|c|} \hline & & & \\ \hline & & & \\ \hline & & & \\ \hline \end{array} \quad 6 + 3t \\
 \begin{array}{|c|c|c|c|} \hline & & & \\ \hline & & & \\ \hline & & & \\ \hline \end{array} \quad 11 + 2t \\
 \begin{array}{|c|c|c|c|} \hline & & & \\ \hline & & & \\ \hline & & & \\ \hline \end{array} \quad 0
 \end{array}$$

- Configuration is conserved (action variable)
 - Rigging flows linearly (angle variable)
 - KKR bijection linearizes the dynamics (direct/inverse scattering map)

How does the BBS dynamics look like in terms of rigged configurations ?

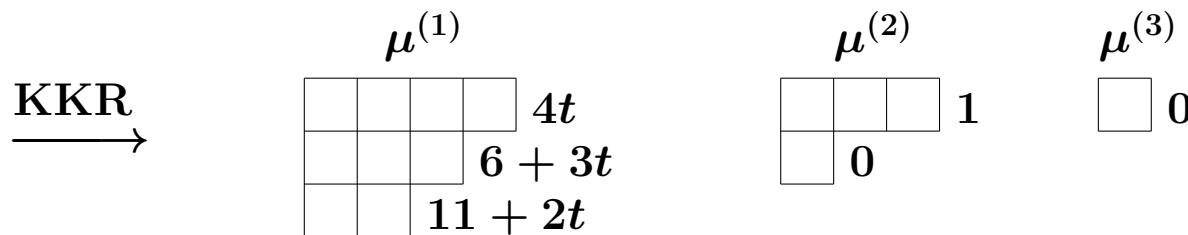
$t = 0:$ 0000**1111000002210032**00000000000000000000000000000000000000
 $t = 1:$ 00000000**11110000221032**0000000000000000000000000000000000000
 $t = 2:$ 000000000000**111100022132**0000000000000000000000000000000000000
 $t = 3:$ 0000000000000000**11110021322**00000000000000000000000000000000000
 $t = 4:$ 000000000000000000000000**1110211322**0000000000000000000000000000000
 $t = 5:$ 00000000000000000000000000**11002113221**00000000000000000000000000000
 $t = 6:$ 0000000000000000000000000000**1100021103221**0000000000000000000000000
 $t = 7:$ 000000000000000000000000000000**110000211003221**00000000000000000000000



- Configuration is conserved (action variable)
- Rigging flows linearly (angle variable)
- KKR bijection linearizes the dynamics (direct/inverse scattering map)

Rigged configuration = action angle variable of BBS!

How does the BBS dynamics look like in terms of rigged configurations ?



- Configuration is conserved (action variable)
 - Rigging flows linearly (angle variable)
 - KKR bijection linearizes the dynamics (direct/inverse scattering map)

Rigged configuration = action angle variable of BBS!

$\mu^{(1)}$ = list of amplitude of solitons (Soliton/String correspondence)
 $(\mu^{(1)}, \dots, \mu^{(n)})$ will be called a **soliton content**.

Randomized box-ball system

$$\begin{array}{ccc} \text{BBS state} & & \text{Soliton content} \\ i_1 i_2 \dots i_L 00000 \dots & \xrightarrow{\text{KKR}} & (\mu^{(1)}, \dots, \mu^{(n)}) \end{array}$$

Randomize $i_1 i_2 \dots i_L$ by introducing the i.i.d. measure on the set of states:

$$\text{Prob}(\text{local state} = i) = p_i \quad (p_0 + \dots + p_n = 1).$$

Randomized box-ball system

$$\begin{array}{ccc} \text{BBS state} & & \text{Soliton content} \\ i_1 i_2 \dots i_L 00000 \dots & \xrightarrow{\text{KKR}} & (\mu^{(1)}, \dots, \mu^{(n)}) \end{array}$$

Randomize $i_1 i_2 \dots i_L$ by introducing the i.i.d. measure on the set of states:

$$\text{Prob}(\text{local state} = i) = p_i \quad (p_0 + \dots + p_n = 1).$$

Limit shape Problem

Determine the **scaling form** of the most probable $(\mu^{(1)}, \dots, \mu^{(n)})$ when $L \rightarrow \infty$.

Randomized box-ball system

$$\begin{array}{ccc} \text{BBS state} & & \text{Soliton content} \\ i_1 i_2 \dots i_L 00000 \dots & \xrightarrow{\text{KKR}} & (\mu^{(1)}, \dots, \mu^{(n)}) \end{array}$$

Randomize $i_1 i_2 \dots i_L$ by introducing the i.i.d. measure on the set of states:

$$\text{Prob}(\text{local state} = i) = p_i \quad (p_0 + \dots + p_n = 1).$$

Limit shape Problem

Determine the **scaling form** of the most probable $(\mu^{(1)}, \dots, \mu^{(n)})$ when $L \rightarrow \infty$.

This can be done by **TBA** minimizing the free energy F associated with

$$\text{Prob}(\mu^{(1)}, \dots, \mu^{(n)}) \propto e^{-\beta_1 |\mu^{(1)}| - \dots - \beta_n |\mu^{(n)}|} \prod_{a=1}^n \prod_{i \geq 1} \binom{h_i^{(a)} + m_i^{(a)}}{m_i^{(a)}},$$

$$e^{\beta_a} := p_{a-1}/p_a,$$

Introduce the scaled string and hole densities $\rho_i^{(a)}, \sigma_i^{(a)}$ by

$$m_i^{(a)} \simeq L \rho_i^{(a)}, \quad h_i^{(a)} \simeq L \sigma_i^{(a)}, \quad \sigma_i^{(a)} = \delta_{a,1} - \sum_{b=1}^n C_{ab} \sum_{j \geq 1} \min(i, j) \rho_j^{(b)},$$

Assume $p_0 \geq \dots \geq p_n$ in the rest.

The condition $\frac{\delta F}{\delta \rho_i^{(a)}} = 0$ leads to the **TBA equation**

$$-i\beta_a + \log(1 + Y_i^{(a)}) = \sum_{b=1}^n C_{ab} \sum_{j \geq 1} \min(i, j) \log(1 + (Y_j^{(b)})^{-1})$$

in terms of $Y_i^{(a)} = \frac{\sigma_i^{(a)}}{\rho_i^{(a)}}$ with the boundary condition $\lim_{i \rightarrow \infty} \frac{1 + Y_{i+1}^{(a)}}{1 + Y_i^{(a)}} = e^{\beta_a}$.

This is equivalent to the (constant) **Y-system**

$$(Y_i^{(a)})^2 = \frac{(1 + Y_{i-1}^{(a)})(1 + Y_{i+1}^{(a)})}{(1 + (Y_i^{(a-1)})^{-1})(1 + (Y_i^{(a+1)})^{-1})}$$

The condition $\frac{\delta F}{\delta \rho_i^{(a)}} = 0$ leads to the **TBA equation**

$$-i\beta_a + \log(1 + Y_i^{(a)}) = \sum_{b=1}^n C_{ab} \sum_{j \geq 1} \min(i, j) \log(1 + (Y_j^{(b)})^{-1})$$

in terms of $Y_i^{(a)} = \frac{\sigma_i^{(a)}}{\rho_i^{(a)}}$ with the boundary condition $\lim_{i \rightarrow \infty} \frac{1 + Y_{i+1}^{(a)}}{1 + Y_i^{(a)}} = e^{\beta_a}$.

This is equivalent to the (constant) **Y-system**

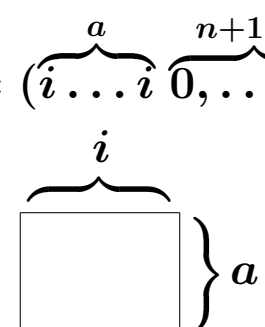
$$(Y_i^{(a)})^2 = \frac{(1 + Y_{i-1}^{(a)})(1 + Y_{i+1}^{(a)})}{(1 + (Y_i^{(a-1)})^{-1})(1 + (Y_i^{(a+1)})^{-1})}$$

Solution (Rare case for which an exact formula can be given)

$$Y_i^{(a)} = \frac{Q_{i-1}^{(a)} Q_{i+1}^{(a)}}{Q_i^{(a-1)} Q_i^{(a+1)}},$$

$$Q_i^{(a)} = Q_i^{(a)}(p_0, \dots, p_n) = \frac{\det(p_k^{\lambda_j + n - j})_{j,k=0}^n}{\det(p_k^{n-j})_{j,k=0}^n} \quad ((\lambda_0, \dots, \lambda_n) = (\overbrace{i \dots i}^a \overbrace{0, \dots, 0}^{n+1-a}))$$

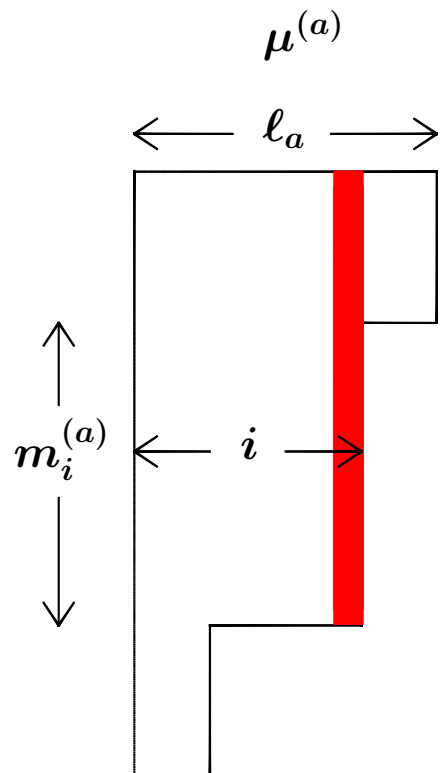
= **Schur function** for $a \times i$ rectangular Young diagram



Result. The limit shape of soliton content $(\mu^{(1)}, \dots, \mu^{(n)})$ is given by

$$\eta_i^{(a)} := \lim_{L \rightarrow \infty} \frac{1}{L} (\text{Length of the } i \text{ th column of } \mu^{(a)}) = \frac{Q_{i-1}^{(a-1)} Q_i^{(a+1)}}{Q_i^{(a)} Q_{i-1}^{(a)} Q_1^{(1)}}$$

$$\text{width } \ell_a \text{ of } \mu^{(a)} \simeq \frac{\log L}{\log \frac{p_{a-1}}{p_a}} \quad (L \rightarrow \infty \text{ if } p_0 > \dots > p_n)$$

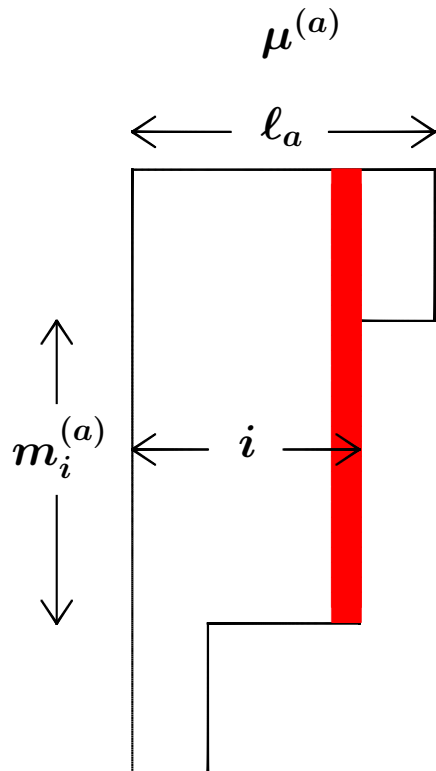


Result. The limit shape of soliton content $(\mu^{(1)}, \dots, \mu^{(n)})$ is given by

$$\eta_i^{(a)} := \lim_{L \rightarrow \infty} \frac{1}{L} (\text{Length of the } i \text{ th column of } \mu^{(a)}) = \frac{Q_{i-1}^{(a-1)} Q_i^{(a+1)}}{Q_i^{(a)} Q_{i-1}^{(a)} Q_1^{(1)}}$$

$$\text{width } \ell_a \text{ of } \mu^{(a)} \simeq \frac{\log L}{\log \frac{p_{a-1}}{p_a}} \quad (L \rightarrow \infty \text{ if } p_0 > \dots > p_n)$$

Special case $p_a = \frac{q^a}{1+q+\dots+q^n}$ ($0 < q \leq 1$).



Scaled column length of $\mu^{(a)}$

$$\eta_i^{(a)} = \frac{q^{i+a-1}(1-q)(1-q^a)(1-q^{n+1-a})}{(1-q^{n+1})(1-q^{i+a-1})(1-q^{i+a})}$$

Strings

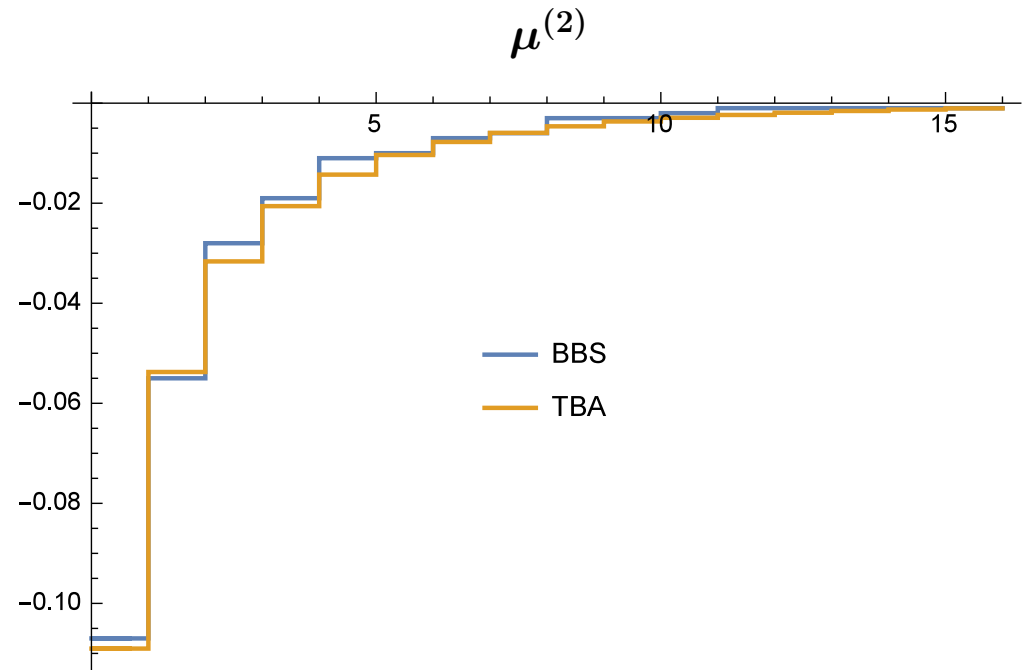
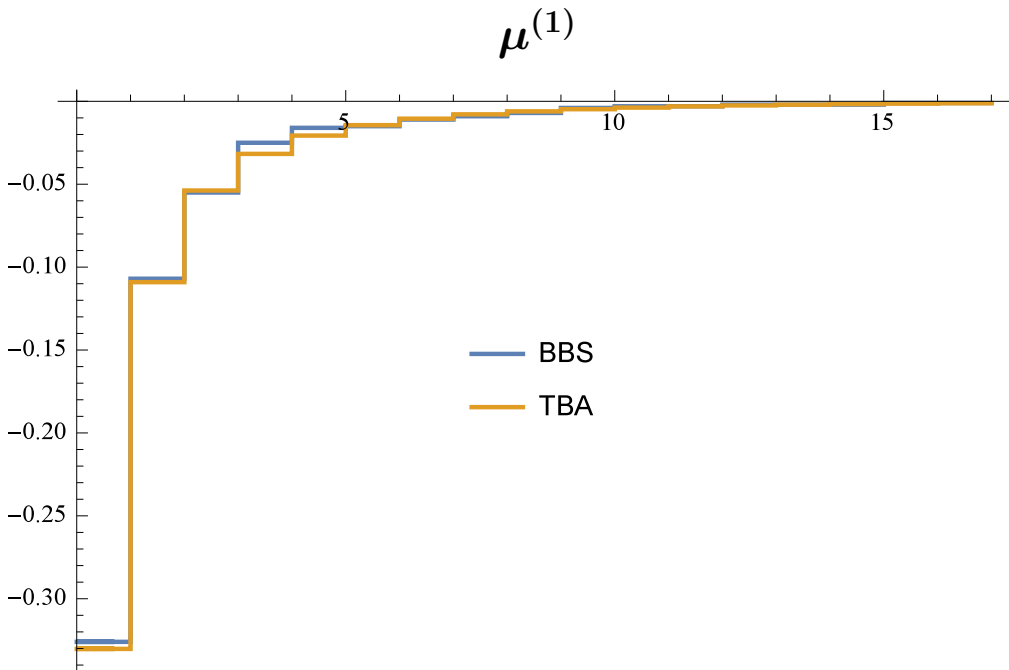
$$\rho_i^{(a)} = \lim_{L \rightarrow \infty} \frac{1}{L} m_i^{(a)} = \frac{q^{i+a-1}(1-q)^2(1-q^a)(1-q^{n+1-a})(1+q^{i+a})}{(1-q^{n+1})(1-q^{i+a-1})(1-q^{i+a})(1-q^{i+a+1})}$$

Holes

$$\sigma_i^{(a)} = \lim_{L \rightarrow \infty} \frac{1}{L} h_i^{(a)} = \frac{q^{a-1}(1-q)^2(1-q^i)(1-q^{n+i+1})(1+q^{i+a})}{(1-q^{n+1})(1-q^{i+a-1})(1-q^{i+a})(1-q^{i+a+1})}$$

2-color BBS with $L = 1000$ sites with distribution $(p_0, p_1, p_2) = (\frac{7}{18}, \frac{6}{18}, \frac{5}{18})$.

Vertically L^{-1} scaled soliton contents.



Generalized hydrodynamics, GHD (from here 1-color BBS only)

[Castro-Alvaredo, Doyon, Yoshimura, Bertini, Collura, De Nardis, Fagotti, ... 2016~]

Densities: ρ_i (i -soliton), σ_i (i -hole), $(\rho_i, \sigma_i) = (\rho_i^{(1)}, \sigma_i^{(1)})$ in previous pages

Speed equation: $v_i = i + \sum_j 2 \min(i, j)(v_i - v_j)\rho_j$ $\begin{array}{l} v_i = \text{effective speed} \\ 2 \min(i, j) = \text{phase shift} \end{array}$
[Croydon,Sasada]

Solution for homogeneous BBS : $v_i = i \frac{1+q}{1-q} - \frac{2q(1+q)(1-q^i)}{(1-q)^2(1+q^{i+1})}$

Generalized hydrodynamics, GHD (from here 1-color BBS only)

[Castro-Alvaredo, Doyon, Yoshimura, Bertini, Collura, De Nardis, Fagotti, ... 2016~]

Densities: ρ_i (i -soliton), σ_i (i -hole), $(\rho_i, \sigma_i) = (\rho_i^{(1)}, \sigma_i^{(1)})$ in previous pages

Speed equation: $v_i = i + \sum_j 2 \min(i, j)(v_i - v_j)\rho_j$ $\begin{pmatrix} v_i = \text{effective speed} \\ 2 \min(i, j) = \text{phase shift} \end{pmatrix}$
 [Croydon,Sasada]

$$\text{Solution for homogeneous BBS : } v_i = i \frac{1+q}{1-q} - \frac{2q(1+q)(1-q^i)}{(1-q)^2(1+q^{i+1})}$$

GHD: assumes weak (x, t) dependence of ρ_i, σ_i ,
 postulates continuity equation and local entropy maximum

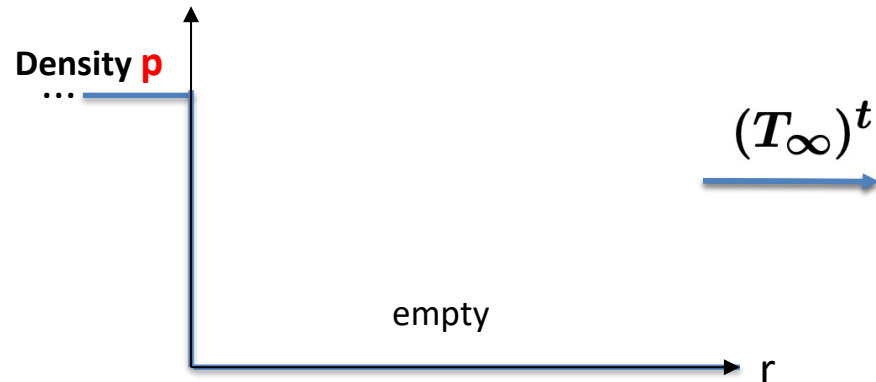
\Rightarrow **Y-variable** $Y_i := \frac{\rho_i}{\sigma_i}$ plays the role of **normal mode** satisfying
 the separated equation $\frac{\partial Y_i}{\partial t} + v_i \frac{\partial Y_i}{\partial x} = 0$ for each i .

One of its most fruitful application is the Riemann problem:

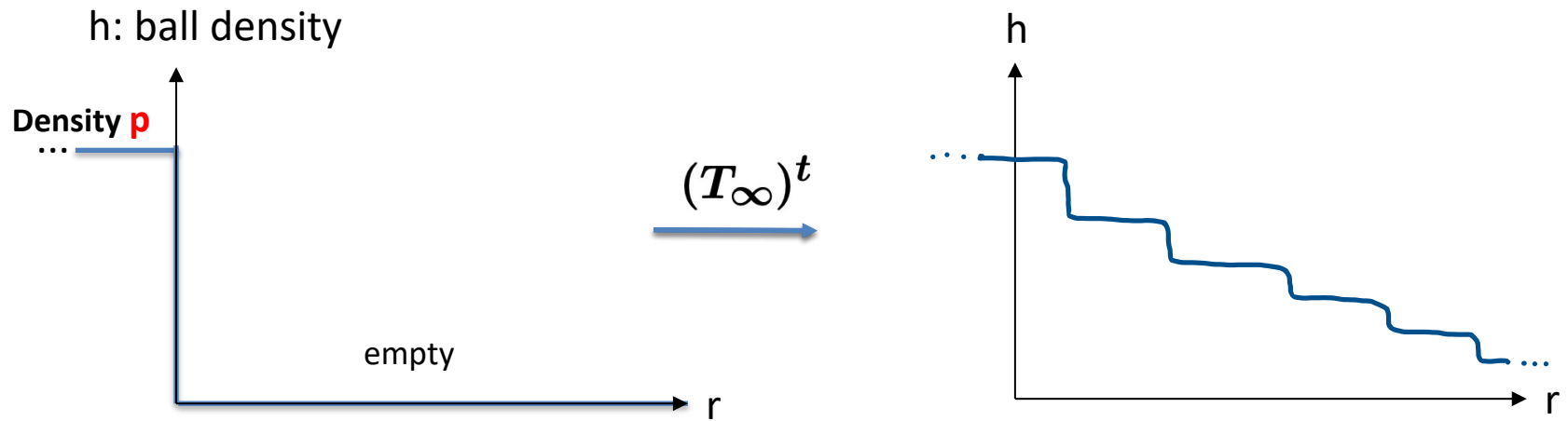
“Describe the profile of the fluid starting from the *homogeneous* initial state except a *single discontinuity* at some point.”

Density Plateaux emerging from domain wall initial condition

h : ball density

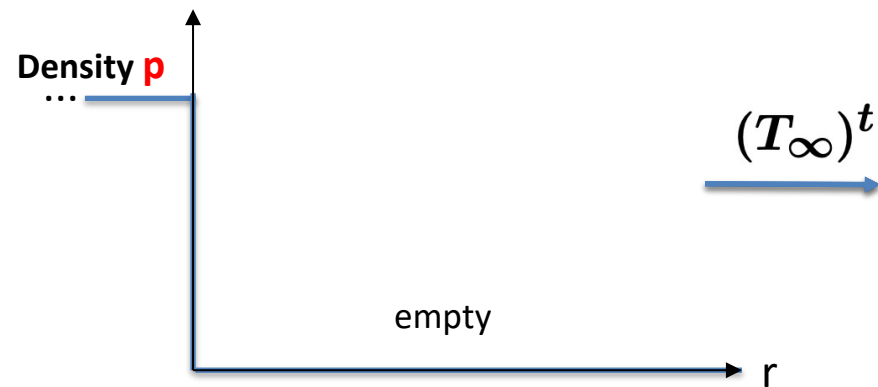


Density Plateaux emerging from domain wall initial condition

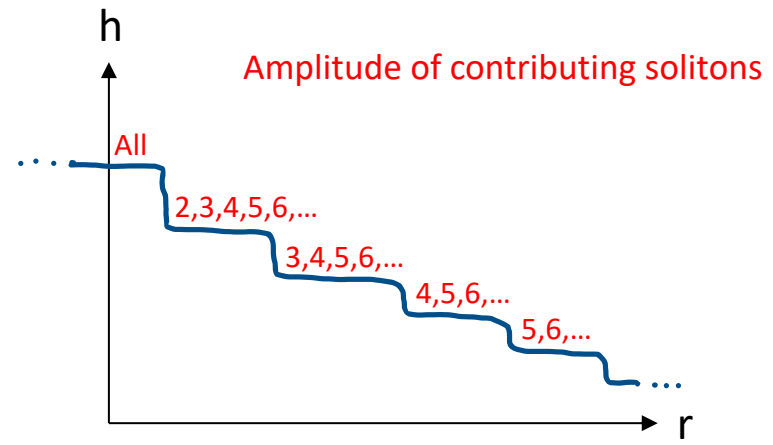


Density Plateaux emerging from domain wall initial condition

h : ball density

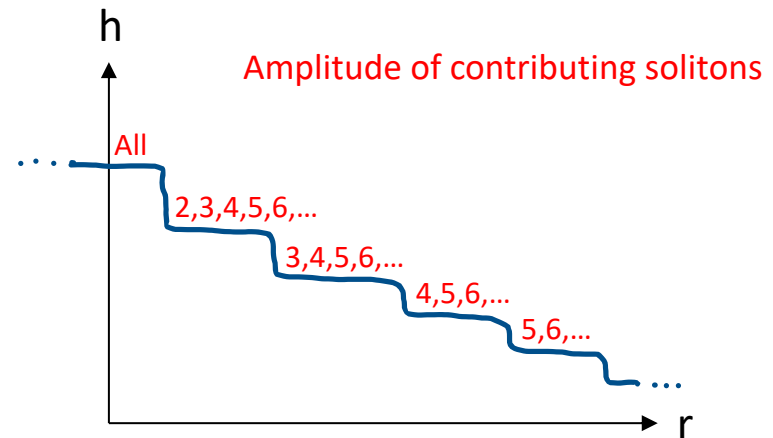
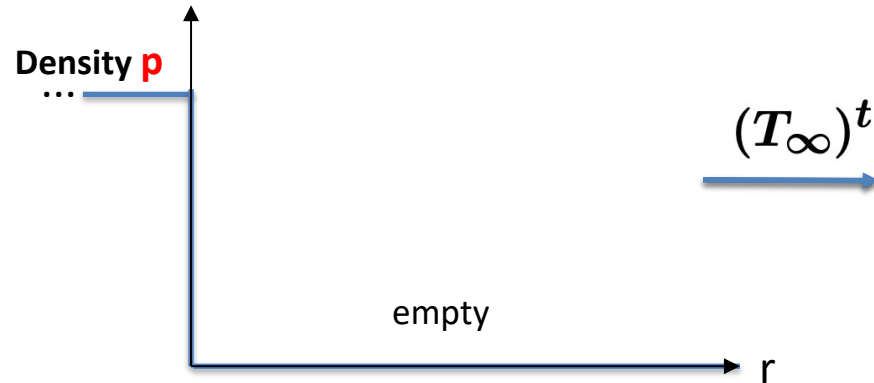


Amplitude of contributing solitons

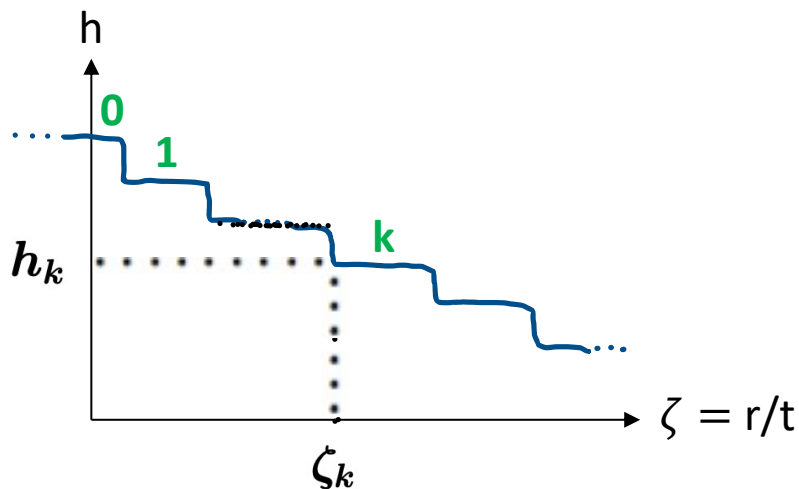


Density Plateaux emerging from domain wall initial condition

h : ball density

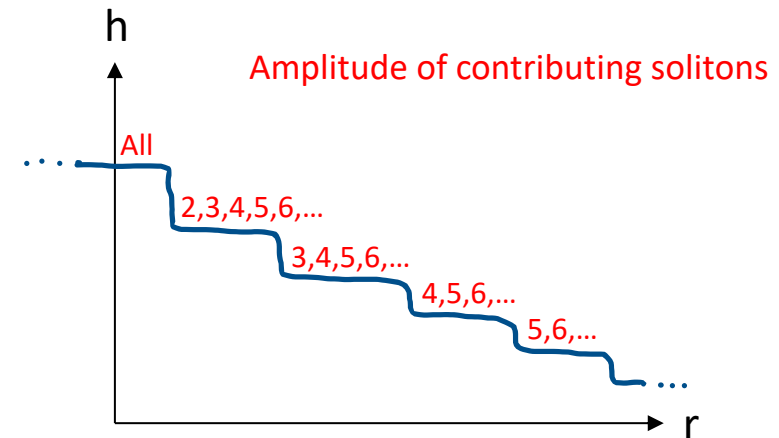
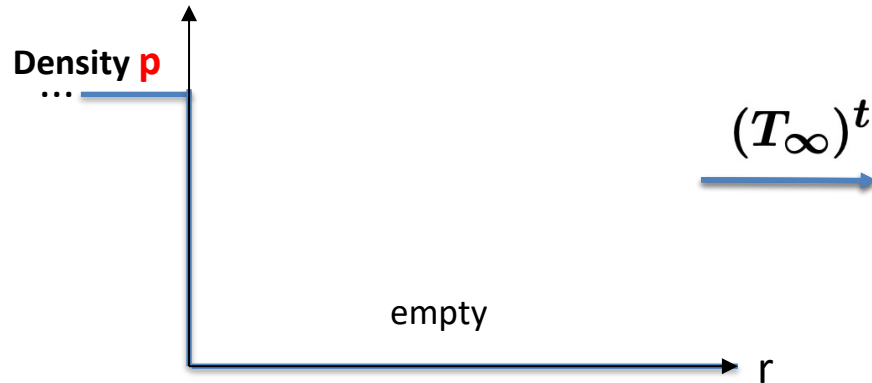


Plateaux grow linearly in time t . The plot against $\zeta = r/t$ collapses into a single curve.

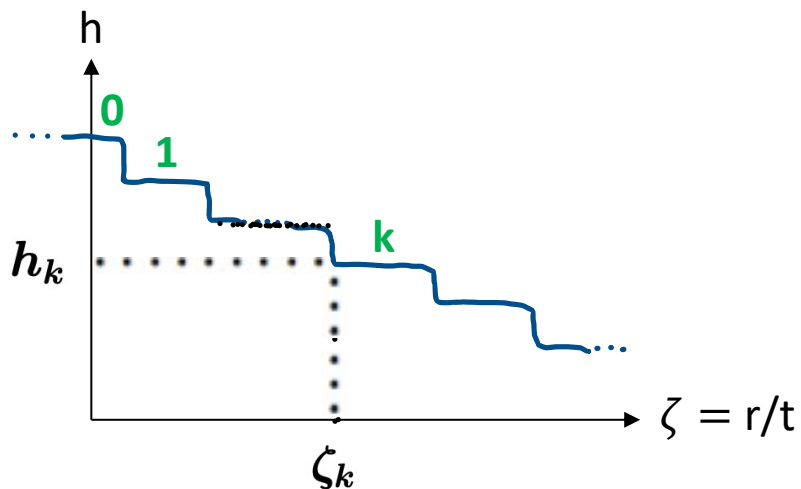


Density Plateaux emerging from domain wall initial condition

h : ball density



Plateaux grow linearly in time t . The plot against $\zeta = r/t$ collapses into a single curve.



GHD prediction

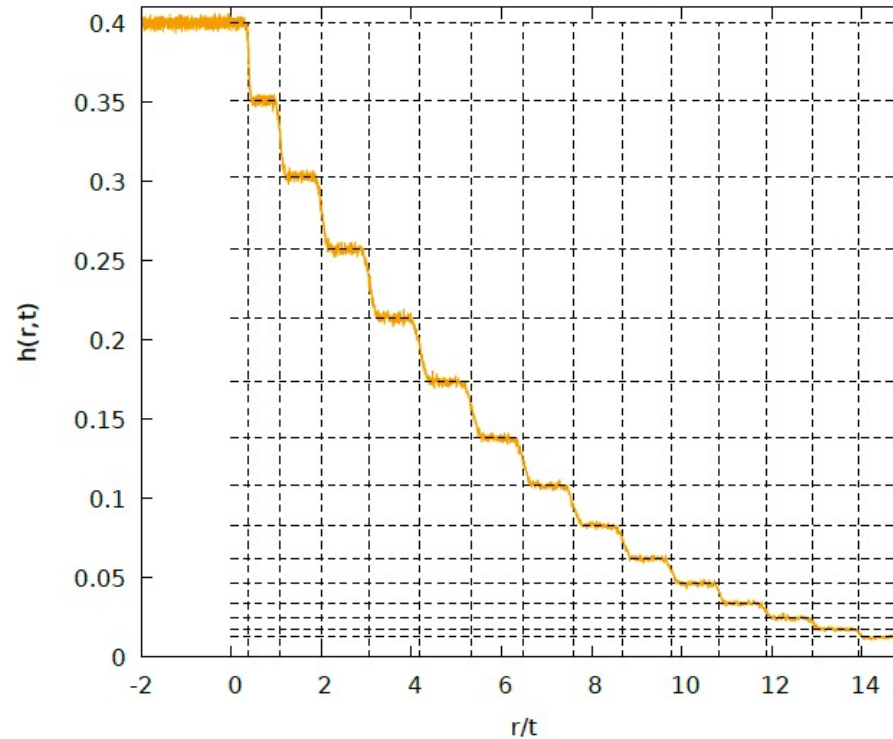
$$h_k = \frac{q^{k+1}(1 - q^{k+2} + k(1 - q))}{1 - q^{2k+3} + (2k + 1)(1 - q)q^{k+1}}$$

$$\zeta_k = \frac{k(1 - q^{k+1})}{1 + q^{k+1}} \quad \left(p = \frac{q}{1 + q} \right)$$

Simulation with $N_{\text{samples}} = 50000$

(Plots of ball density vs $\zeta = r/t$. Dotted lines are GHD predictions)

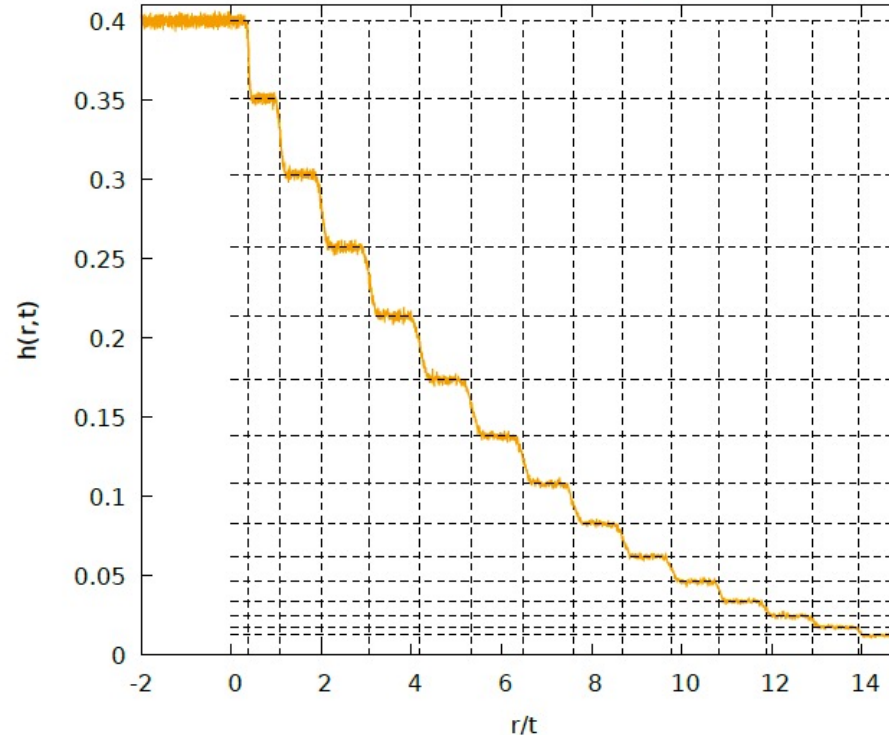
$p=0.4$, $q=0.666\dots$, $t=500$.



Simulation with $N_{\text{samples}} = 50000$

(Plots of ball density vs $\zeta = r/t$. Dotted lines are GHD predictions)

$p=0.4$, $q=0.666\dots$, $t=500$.



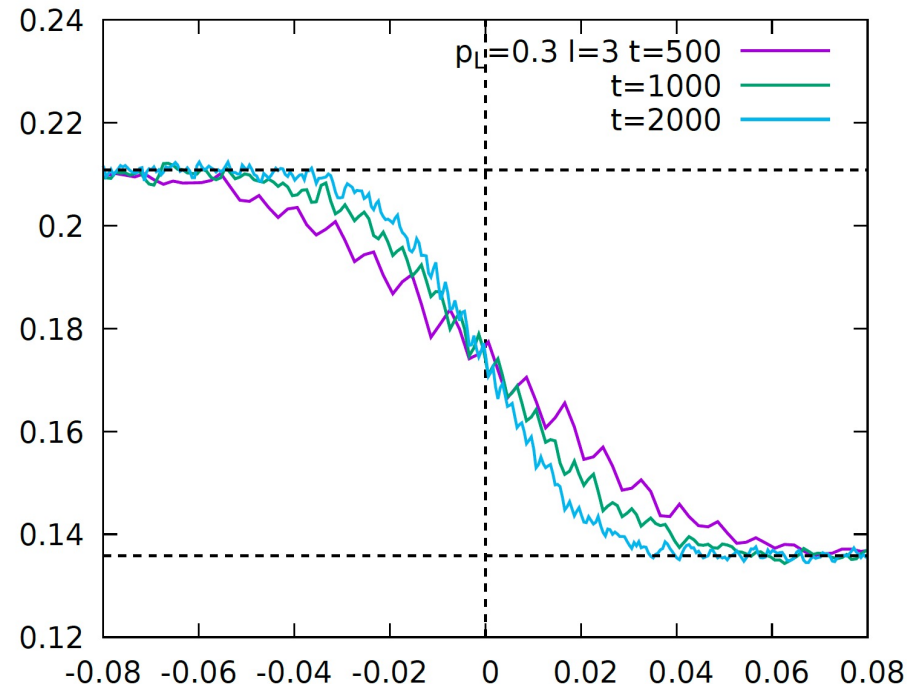
Actual plateau edges are not strict and exhibit some **broadening**.

This is due to **diffusive** correction to the **ballistic** picture,
which may be viewed as a finite t effect.

Analytical description of the **diffusive broadening** of plateau edges

Position of plateau edge - ζ
fluctuates over the scale

$$\frac{1}{\sqrt{(\text{Diffusion const})t}}$$

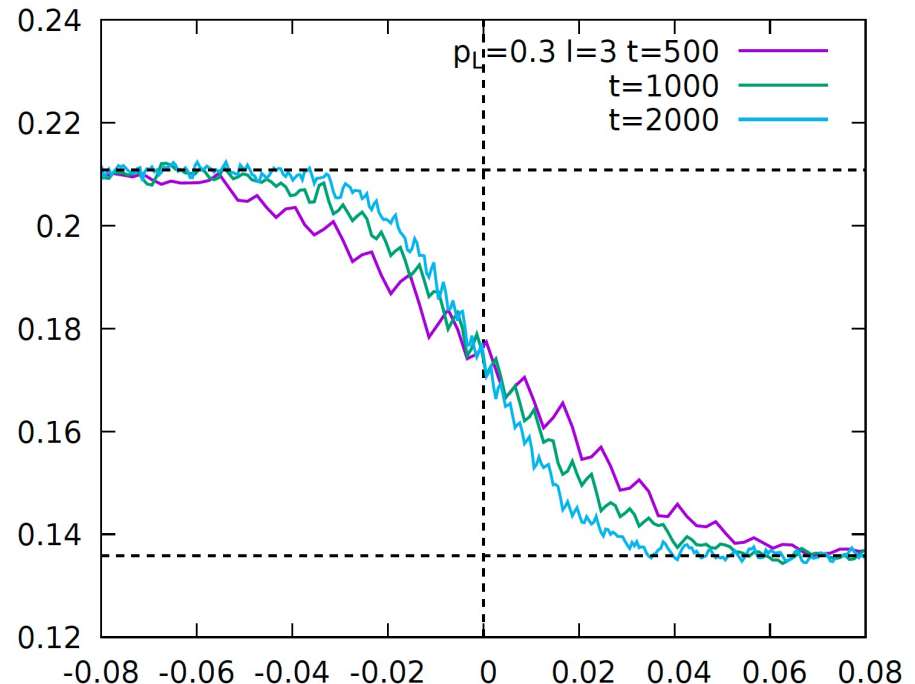


Analytical description of the **diffusive broadening** of plateau edges

Position of plateau edge - ζ
 fluctuates over the scale

$$\frac{1}{\sqrt{(\text{Diffusion const})t}}$$

$$\operatorname{erfc}(u) = \frac{2}{\sqrt{\pi}} \int_u^\infty e^{-s^2} ds$$



$$\langle \rho_j(r, t) \rangle = \frac{1}{2} (\rho_j(k-1) - \rho_j(k)) \operatorname{erfc} \left(\frac{r - \zeta(k)t}{\sqrt{2t} \Sigma_k^{(l)}} \right) + \rho_j(k)$$

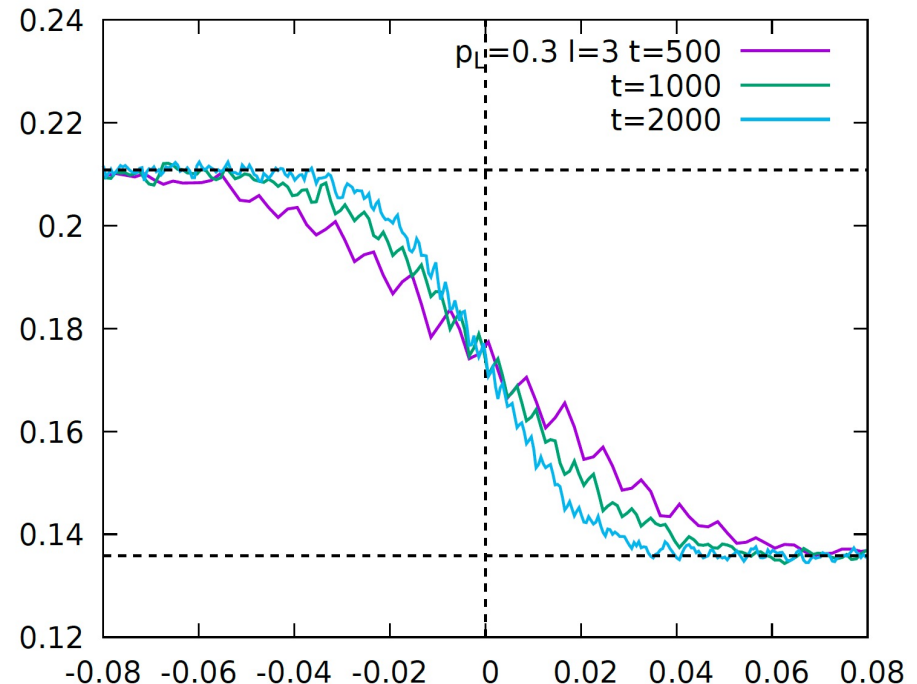
amplitude j -soliton density around the k th plateau edge $r = \zeta(k)t$ under the time evolution T_l .

Analytical description of the **diffusive broadening** of plateau edges

Position of plateau edge - ζ
fluctuates over the scale

$$\frac{1}{\sqrt{(\text{Diffusion const})t}}$$

$$\operatorname{erfc}(u) = \frac{2}{\sqrt{\pi}} \int_u^\infty e^{-s^2} ds$$



$$\langle \rho_j(r, t) \rangle = \frac{1}{2} (\rho_j(k-1) - \rho_j(k)) \operatorname{erfc} \left(\frac{r - \zeta(k)t}{\sqrt{2t} \Sigma_k^{(l)}} \right) + \rho_j(k)$$

amplitude j -soliton density around the k th plateau edge $r = \zeta(k)t$ under the time evolution T_l .

$$(\Sigma_k^{(l)})^2 = \frac{4k^2 q^{k+1} (1 - q^{k+1})(1 - q^{l-k})(1 + q^{l+k+2})}{(1 + q^{k+1})^3 (1 - q^{l+1})^2}$$

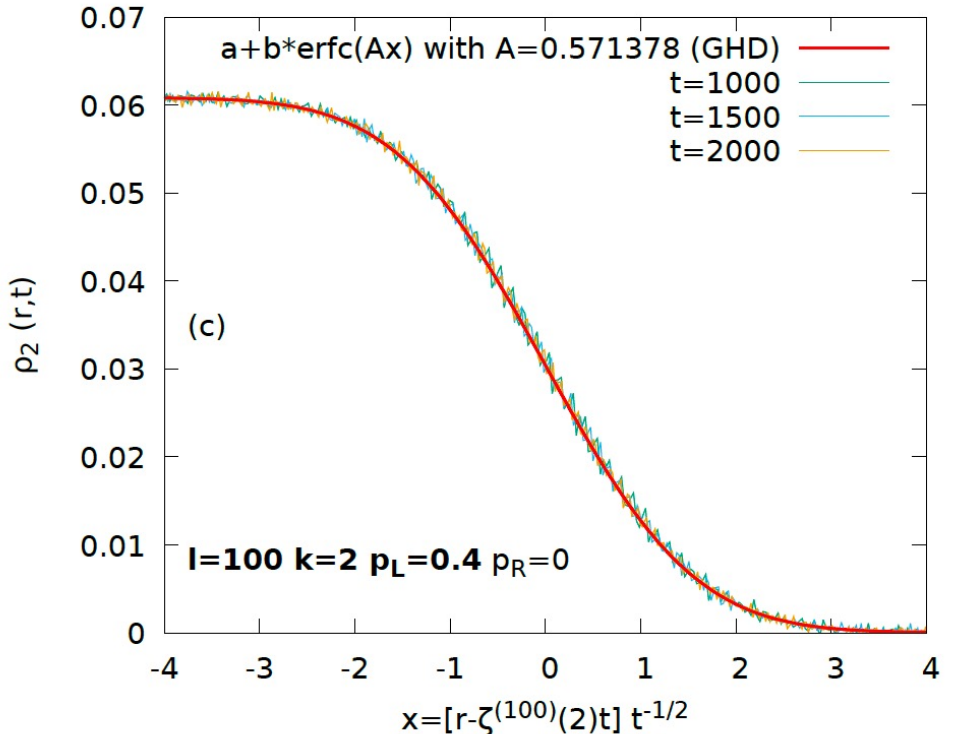
← GHD
(Bethe ansatz)

Analytical description of the **diffusive broadening** of plateau edges

Position of plateau edge - ζ
fluctuates over the scale

$$\frac{1}{\sqrt{(\text{Diffusion const})t}}$$

$$\operatorname{erfc}(u) = \frac{2}{\sqrt{\pi}} \int_u^\infty e^{-s^2} ds$$



$$\langle \rho_j(r, t) \rangle = \frac{1}{2} (\rho_j(k-1) - \rho_j(k)) \operatorname{erfc} \left(\frac{r - \zeta(k)t}{\sqrt{2t} \Sigma_k^{(l)}} \right) + \rho_j(k)$$

amplitude j -soliton density around the k th plateau edge $r = \zeta(k)t$ under the time evolution T_l .

$$(\Sigma_k^{(l)})^2 = \frac{4k^2 q^{k+1} (1 - q^{k+1})(1 - q^{l-k})(1 + q^{l+k+2})}{(1 + q^{k+1})^3 (1 - q^{l+1})^2}$$

← GHD
(Bethe ansatz)

Current fluctuation and Large deviation

N_t = number of balls crossing $x = 0$ during time interval $[0, t]$.

Scaled cumulant generating function under time evolution T_l :

$$\begin{aligned} F(\lambda) &= \lim_{t \rightarrow \infty} \frac{1}{t} \log \langle e^{\lambda N_t} \rangle = \sum_{k=1}^{\infty} \frac{\lambda^k}{k!} \left(\lim_{t \rightarrow \infty} \frac{1}{t} \langle N_t^k \rangle^c \right) \\ &= \log \left(\frac{1 - (qe^\lambda)^{l+1}}{1 - qe^\lambda} \right) - \log \left(\frac{1 - q^{l+1}}{1 - q} \right) \end{aligned}$$

Current fluctuation and Large deviation

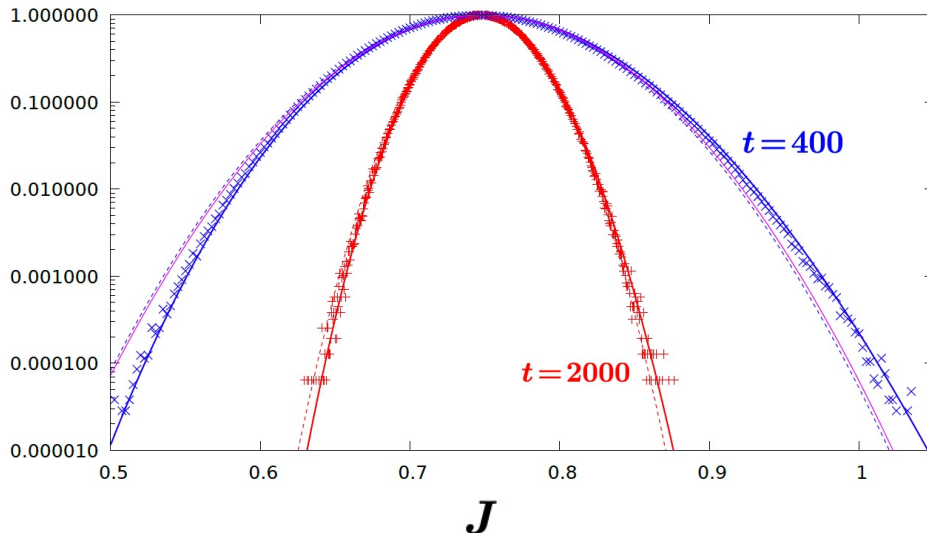
N_t = number of balls crossing $x = 0$ during time interval $[0, t]$.

Scaled cumulant generating function under time evolution T_l :

$$\begin{aligned} F(\lambda) &= \lim_{t \rightarrow \infty} \frac{1}{t} \log \langle e^{\lambda N_t} \rangle = \sum_{k=1}^{\infty} \frac{\lambda^k}{k!} \left(\lim_{t \rightarrow \infty} \frac{1}{t} \langle N_t^k \rangle^c \right) \\ &= \log \left(\frac{1 - (qe^\lambda)^{l+1}}{1 - qe^\lambda} \right) - \log \left(\frac{1 - q^{l+1}}{1 - q} \right) \end{aligned}$$

Large deviation rate function:

$$G(J) = \text{Legendre transformation of } F(\lambda)$$



Plot : $\frac{\text{Prob}(N_t/t = J)}{\text{Prob}_{\max}}$ ($10^{6.5}$ samples)

Solid curves: $\exp(-tG(J))$

Dotted curves: Gaussian fit

(ball density = 0.3, time evolution = T_{10})

Current fluctuation and Large deviation

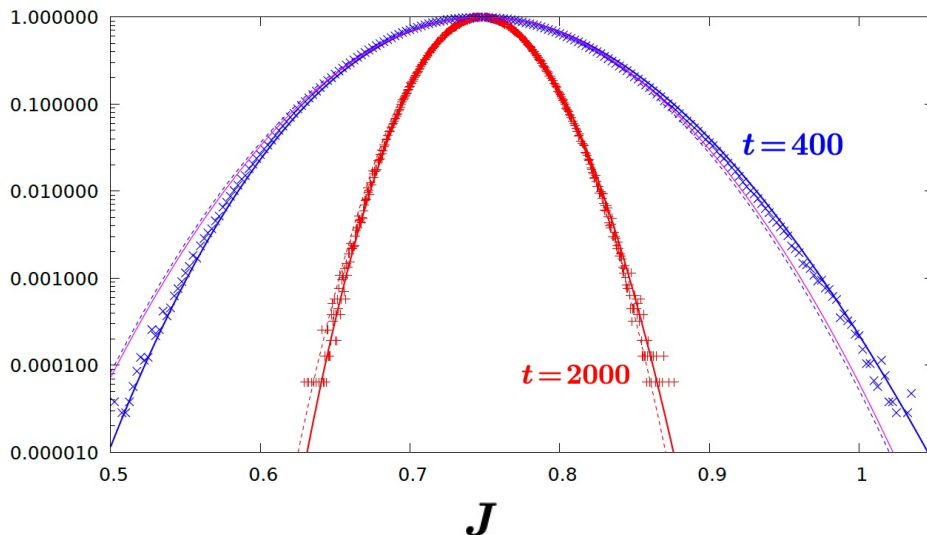
N_t = number of balls crossing $x = 0$ during time interval $[0, t]$.

Scaled cumulant generating function under time evolution T_l :

$$\begin{aligned} F(\lambda) &= \lim_{t \rightarrow \infty} \frac{1}{t} \log \langle e^{\lambda N_t} \rangle = \sum_{k=1}^{\infty} \frac{\lambda^k}{k!} \left(\lim_{t \rightarrow \infty} \frac{1}{t} \langle N_t^k \rangle^c \right) \\ &= \log \left(\frac{1 - (qe^\lambda)^{l+1}}{1 - qe^\lambda} \right) - \log \left(\frac{1 - q^{l+1}}{1 - q} \right) \end{aligned}$$

Large deviation rate function:

$$G(J) = \text{Legendre transformation of } F(\lambda)$$



Plot : $\frac{\text{Prob}(N_t/t = J)}{\text{Prob}_{\max}} (10^{6.5} \text{ samples})$

Solid curves: $\exp(-tG(J))$

Dotted curves: Gaussian fit

(ball density = 0.3, time evolution = T_{10})

F and G have been obtained also for non-i.i.d. 2-temperature GGE

Summary

1. BBS is a Yang-Baxter integrable cellular automaton with quantum group symmetry and explicit action-angle variables originating in Bethe strings.
2. Limit shape of soliton content in randomized BBS is determined by TBA.
3. It serves as an essential input to GHD, which provides an analytical description of the density plateaux emerging from domain wall initial conditions and the large deviation principle of the current.

Reference

Review part:

Inoue-K-Takagi

Integrable structure of box-ball systems: crystal, Bethe ansatz,
ultradiscretization and tropical geometry, JPA Topical Review (2012)

Limit shape problem:

K-Lyu-Okado

Randomized box-ball systems, limit shape of rigged configurations and
thermodynamic Bethe ansatz, NPB(2018)

Generalized hydrodynamics of BBS:

K-Misguich-Pasquier,

Generalized hydrodynamics in box-ball system, JPA(2020)

Generalized hydrodynamics in complete box-ball system for $U_q(\widehat{sl}_n)$, SciPostPhys (2021)

Current fluctuations and large deviations in a box-ball system, in preparation